



Effects of pairwise, donor–acceptor functional groups on polymer solubility, solution viscosity and mist control

R.L. Ameri David, Ming-Hsin Wei, Julia A. Kornfield*

Division of Chemistry and Chemical Engineering, California Institute of Technology, Pasadena, California 91125, USA

ARTICLE INFO

Article history:

Received 19 June 2009

Received in revised form

29 September 2009

Accepted 3 October 2009

Available online 11 November 2009

Keywords:

Donor–acceptor interactions

Extensional rheology

Mist control

ABSTRACT

Homologous series of functionalized polymers were used to compare the solution properties of donor–acceptor (DA) interpolymer mixtures with those of self-associating and non-associating polymer analogues. Polymer analogous synthesis was used to produce a series of polymers from a specific, anionically-polymerized prepolymer (1250 kg/mol polybutadiene), using thiol-ene coupling to incorporate systematically-varied contents of side groups: either tertiary amines (as proton acceptors) or carboxylic acids (both as proton donors in donor–acceptor mixtures, or as self-associating moieties in single-polymer solutions). Comparison with controls reveals that, relative to the effects of self-associations, DA interpolymer interactions more strongly affect solution properties such as phase behavior, interpolymer aggregation, shear viscosity, and elastic response in extensional flow. Specifically, DA associations lead to (i) greater reductions in polymer solubility in hydrocarbon solvents, (ii) interpolymer aggregation into larger clusters, and (iii) greater shear viscosity in solution. Nevertheless, DA associations *reduced* solution elasticity and mist suppression—a highly unanticipated result in light of the prior literature.

© 2009 Published by Elsevier Ltd.

1. Introduction

Polymer additives are widely used to modify droplet dynamics and turbulent flow behavior of fluids. It is known that ultra-high molar mass polymers are particularly effective in controlling drop size distribution in sprays, deposition of droplets on surfaces, and drag reduction, and that their efficacy originates in polymer viscoelasticity and correlates with enhancement of extensional viscosity [1–21] (refer to Appendix A for a more detailed report). Unfortunately, linear chains that are long enough to powerfully influence fluid behavior even at dilute concentrations ($M_w \sim 10^7$ g/mol according to Chao and coworkers [14,22]) undergo scission in turbulent flow (as is manifested, for instance, in the decrease in drag reduction activity with distance along a pipe segment [8]). Therefore, an unmet challenge is to develop an additive that will behave like ultra-long linear chains even after the carrier fluid has been transported, stored, and filtered.

The most promising strategies emerging from the era of intensive effort on antimisting kerosene use polymers that associate with one another via functional groups (termed “stickers”) statistically distributed along the chains [23–25], either with self-

associating groups (Fig. 1a) or with complementary associating groups (Fig. 1b). It has been suggested that associating polymers (i.e., interacting through non-covalent bonds) may provide mist-control additives with superior shear stability (enabled by sacrificing non-covalent linkages during intense flows). Previously [26], we examined self-associating chains (1250 kg/mol polybutadienes functionalized with carboxylic acid side groups) in dilute solutions: intrachain pairing of the stickers led to chain collapse (Fig. 1a, right) and, consequently, to reduced efficacy for mist suppression. In the present study, we test the concept that complementary functional groups (Fig. 1b) could overcome the problems of intramolecular sticker pairing and improve control of fluid breakup (a question conspicuously unresolved in the prior literature). This work has been motivated in part by evidence that mixing two polymers bearing complementary proton-accepting and proton-donating groups leads to the formation, even in dilute solutions, of interpolymer complexes (Fig. 1b, right) that exhibit improved shear-stability [24,25,27].

To elucidate the relevant physical phenomena, we designed and synthesized chains of matched length and length distribution (using polymer analogous synthesis starting from an anionic 1250 kg/mol 1,4-polybutadiene). Homologous series were prepared by functionalizing this prepolymer to create “donor chains” bearing carboxylic acid groups (H-bond donors) and “acceptor chains” with tertiary amine groups (H-bond acceptors). These polymers were

* Corresponding author. Tel.: +1 626 395 4138; fax: +1 626 568 8743.

E-mail address: jak@cheme.caltech.edu (J.A. Kornfield).

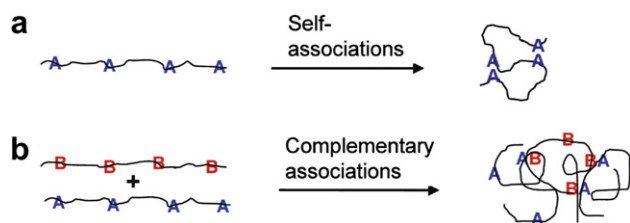


Fig. 1. Schematic diagrams and behavior of flexible chains bearing randomly-placed, pairwise associating functional groups: (a) “self-associating” groups form predominantly intramolecular pairs in dilute solution, and (b) mixtures of donor-functionalized and acceptor-functionalized chains form intermolecular pairs.

used to gain fundamental insight into the molecular design of associative polymers to improve control of drop breakup.

The polymer structures and solution conditions investigated here were chosen to be compatible with the requirements of a polymer additive for improving the fire safety of jet fuel (e.g., maintaining a homogeneous single phase, maintaining low shear viscosity, enhancing extensional viscosity, and suppressing drop breakup). Polybutadiene polymers were chosen because of their solubility in hydrocarbon fuels, ease of functionalization [28], and availability both as commodity polymers and as well-defined, research-grade materials. The chain length was chosen to be long enough to confer significant elasticity [14], yet short enough to avoid chain scission at high shear rates [8]. Hence, chains of $M_w \sim 10^6$ g/mol were examined. To minimize the effects of chain collapse [29–32] and maintain a low shear viscosity [29–34], experiments focused on low extents of functionalization and dilute concentrations, $c < c^*$. The choice of solvent profoundly affects the solubility of the functionalized polymers and of their complexes [26,29]; therefore, it is necessary to perform experiments in the solvent system in which the polymers will be used—here, aviation fuel, specifically Jet-A. To expose the molecular basis of the macroscopic properties of these solutions, we systematically studied the effects of the degrees of functionalization of donor and acceptor chains, the overall polymer concentration, and the ratio of donor and acceptor chains.

The present contribution augments the existing state of knowledge concerning the effects of intermolecular donor–acceptor interactions on polymer solution properties [35].

2. Experimental

2.1. Materials

Prepolymer PB chains of $M_w = 1250$ kg/mol, hereafter referred to as 1250kPB, were purchased from Polymer Source, Inc. (product ID P1914-Bd, containing $\sim 8\%$ 1,2 adducts, with $M_w/M_n = 1.09$). Polyisobutylene of $M_w = 4200$ kg/mol, hereafter referred to as 4200kPIB, was purchased from Aldrich (product number 181498, with $M_w/M_n = 1.35$). 2,6-Di-*tert*-butyl-4-methylphenol (BHT), 3-mercaptopropionic acid (MPA), 2-(dimethyl-amino)ethanethiol hydrochloride (DMAET), and 2,2'-Azobis(2-ethylpropionitrile) (AIBN) were obtained at 99% purity from Sigma–Aldrich (except for DMAET, obtained at 95% purity). AIBN was recrystallized biweekly in methanol (10 mL solvent per g AIBN) and stored at 4 °C; all other reagents were stored at room temperature and used as received without further purification.

Jet-A was purchased from a small local airport. A kerosene-type aviation fuel, Jet-A is a mixture of a large number of different hydrocarbons (including paraffins, iso-paraffins, aromatics, and naphthalene) of carbon number C5–C20 (with dominant contribution from C10–C14 species). Although the precise composition of Jet-A-1 varies, it must not exceed prescribed limits on content of

water, acidic groups, and sulfur (among others; see UK specification DEF STAN 91–91, NATO code F-35, and ASTM International Standard Specification D1655–08a).

2.2. Polymer functionalization and characterization

The functionalization of 1250kPB with DMAET was performed according to the following representative procedure. To 1250kPB (0.50 g, 0.74 mmol 1,2-PB repeat units) dissolved in 50 mL of THF in a 100 mL Schlenk flask were added DMAET (0.31 g, 2.1 mmol) and azobisisobutyronitrile (AIBN, 51 mg, 0.31 mmol), both dissolved in a mixture of 5 mL THF and 5 mL methanol. The contents of the Schlenk flask were degassed in 3 freeze-pump-thaw cycles, warmed to 55 °C, and then allowed to react at 55 °C for 7 h. Following the reaction, the polymer solution was transferred to a 100 mL jar containing a small amount of 2,6-di-*tert*-butyl-4-methylphenol (BHT), concentrated by evaporation of all but the last 20 mL solvent under an argon stream, and titrated by addition of potassium hydroxide (0.31 g at 88%, 4.9 mmol, dissolved in a $\sim 1:3:6$ water:methanol:THF solution). The solution was cooled in liquid nitrogen and precipitated by addition of 50 mL of cold methanol. Final purification of the polymer was achieved by reprecipitating twice from a THF solution (containing ca. 1 wt% BHT), first with 50:50 methanol:water and then again with cold methanol, followed by drying to constant weight under vacuum at room temperature. Reaction conditions and results are summarized in Table 1, and results of product characterization by ^1H NMR are shown in Fig. 2.

Acid-functionalized 1250 kg/mol 1,4-PB chains used in this study were the same as those used in an earlier study (Ref. [26], Table 1). The characterization of functionalized polymer by ^1H NMR (to determine the extent of incorporation of MPA and DMAET functional groups) and by gel permeation chromatography (to determine the polymer molecular weight distributions) was performed as documented in Ref. [26].

2.3. Sample preparation and measurements

2.3.1. Sample preparation

Dilute mixtures of acid-functionalized and amine-functionalized polymer were prepared from stock solutions of the individual polymers by mixing in appropriate ratios to obtain target concentrations. Stock solutions were prepared by combining polymer and

Table 1
Reaction Conditions^a and Results for Functionalization of 1250 kg/mol 1,4-Polybutadiene.

Entry ^b	[PB] (g/mL)	[RSH] ^c	[AIBN] (mg/mL)	Rxn time (h)	Funct. ^d %	PDI
1250kPB1.5N	0.008	2.8	0.86	7.0	1.5	–
1250kPB2.6N ^e	0.011	13	1.1	11 ^g	2.6	–
1250kPB5.4N	0.009	20	1.1	12 ^h	5.4	–
1250kPB0.2A ^f	0.010	12	0.46	0.58	0.2	~ 1.15
1250kPB0.3A	0.009	16	0.62	0.55	0.3	~ 1.15
1250kPB0.4A	0.009	16	0.52	1.1	0.4	~ 1.15
1250kPB0.6A	0.009	16	0.54	1.2	0.6	~ 1.15

^a In all cases, reactions were run in THF for functionalization with MPA, and $\sim 9:1$ THF: methanol for functionalization with DMAET.

^b Functionalized PB polymers were named so that the prefix corresponds to the molecular weight of the precursor chain, and the suffix represents the mol% of monomers bearing functional groups (abbreviated as N for DMAET and A for MPA).

^c In molar equivalent of 1,2-PB units.

^d Molar fraction of functionalized monomers based on the total number of PB monomers (both 1,2 and 1,4 units).

^e ^1H NMR spectrum is shown in Fig. 2.

^f GPC trace is given in Fig. 3 of Ref. [26].

^g Reaction temperature was 50 °C instead of 55 °C.

^h First 9 h at 55 °C and last 3 h at 65 °C.

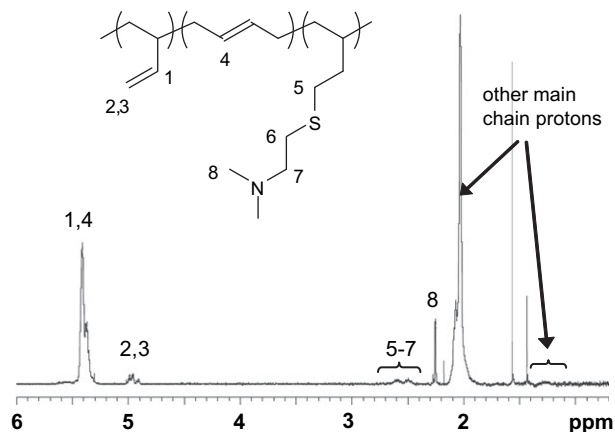


Fig. 2. Representative ^1H NMR spectrum of 1250 kg/mol 1,4-polybutadiene polymer functionalized with 2-(dimethylamino)ethane thiol (1250PB2.6N, refer to Table 1). Visible peaks at $\delta = 2.27$ and 1.43 ppm belong to 2,6-ditertbutyl-4-methylphenol (BHT), and the peak near $\delta \sim 1.6$ ppm corresponds to water.

solvent in clean 20 mL scintillation vials that were placed on a Wrist-Action Shaker (Burrell Scientific) for 6–72 h to allow the polymer to dissolve fully and homogeneously. Polymer samples used for measurements of hydrodynamic diameter by dynamic light scattering were prepared using stock solutions filtered through a $0.4 \mu\text{m}$ pore PTFE membrane with Acrodisc CR 25-mm syringe filters.

2.3.2. Viscosity and size measurements

Shear viscosity measurements were performed under steady-state flow using an AR1000 rheometer (TA Instruments) equipped with a 60 mm diameter, 1° angle, and $29 \mu\text{m}$ truncation aluminum cone geometry. Measurements of apparent polymer hydrodynamic radius in solution were acquired with a ZetaPALS (Brookhaven Instruments) using a laser source with wavelength of 532 nm and collecting the scattered light at an angle of 90° . The built-in Particle Size Software was used to analyze the acquired raw data. Reported apparent hydrodynamic radii represent averages of nine runs of 1 min each.

2.3.3. Characterization of fluid breakup and atomization

The elasticity and relaxation time of polymer solutions under elongational deformation were studied using capillary breakup extensional rheometry using a CaBER1 (Thermo Haake), courtesy of Dr. Jan P. Plog of Thermo Fisher Scientific. The effect of polymer on fluid breakup was characterized using two methods described in an earlier publication [26]: (i) splashing, spreading, and breakup of individual fluid droplets (of size ~ 3 mm) impacting a smooth, solid surface (at velocities of 3 m/s) with the aid of a high-speed, high resolution camera, and (ii) spraying $\sim 1/2$ mL aliquots of fluid with a simple paint gun (at a horizontal angle using 10 psi of air pressure) and visualizing the resulting spray pattern on a horizontal surface 80 cm downstream from the source. (We note that due to the ventilation required when using volatile, flammable solvents, conventional light scattering methods to measure particle size of sprays and aerosols were precluded by excessive variability in the position of the cloud of droplets). Additional information about CaBER, drop breakup, and spray experiments may be found in the Experimental section (including Endnote 17) of Ref. [26].

These three methods were chosen for their complementary advantages given their limitations [26]. Specifically, for the present solutions of 1250kPB in Jet-A (for which $c^* \approx 2500$ ppm by wt), CaBER was restricted to testing of semi-dilute solutions of

$c \geq 1.5$ wt%. On the other hand, droplet impact only led to breakup for very dilute solutions of $c \leq 1000$ ppm. The spray experiment was used across a wide range of concentrations spanning c^* ; however, it was limited to qualitative analysis.

3. Results and discussion

3.1. Functionalized polymers

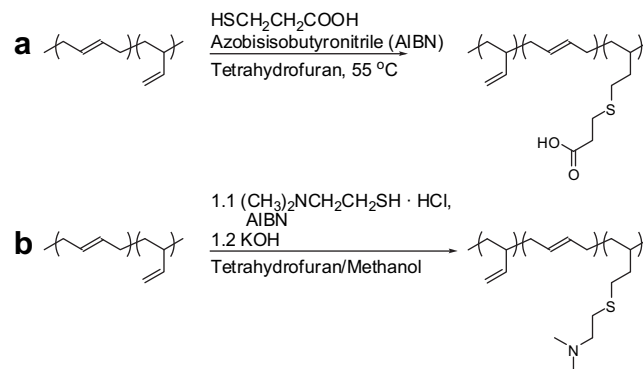
The choice of functionalization of PB by thiol-ene coupling using functional thiols (2-mercaptoethanol and DMAET) was motivated by experience in our lab (consistent with other literature reports, see discussion in Ref. [28]) that this method presents important advantages (relative to other methods such as e.g., hydroboration/oxidation and hydrosilylation) in terms of both experimental convenience and minimal undesirable side-reactions.

3.1.1. Acid-functionalized polybutadiene

Reaction of PB prepolymer according to Scheme 1a using reaction conditions summarized in Table 1 allowed controlled incorporation of carboxylic acid side-groups by radical addition of MPA to the pendant double bonds of 1,2-PB units (Table 1). Consistent with general results for PB modification by thiol-ene coupling under similar conditions, we found that the functionalization reaction occurs with minimal degradation of the precursor material [28]. To maximize the stability of the product polymer and protect it from cross-linking with time, acid-functionalized polybutadienes were stabilized with a small amount of BHT and stored in the dark below 0°C . Under these conditions, polymer crosslinking caused M_w/M_n to increase by <0.1 over time periods of up to 18 months.

3.1.2. Amine-functionalized polybutadiene

Reaction of 1,4-PB (Scheme 1) using the procedure outlined above successfully incorporated tertiary amine side-groups (Table 1, Fig. 2). Given that the addition of other thiols to 1,2-PB and the addition of MPA to 1,4-PB proceed with minimal chain scission or crosslinking (Table 1, Fig. 3 of Ref. [26], Table 1 and Fig. 4 of Ref. [28]), we expected the narrow polydispersity of the 1250kPB starting material to be preserved during the addition reaction of DMAET. Unfortunately, we were not able to assess the MW distribution of the resultant amine-functionalized 1250kPB by gel permeation chromatography: the RI detector output failed to detect a polymer peak (despite the verified presence of polymer in the injected sample), as we had observed with phenol-functionalized 1,2-PB (see entry 92kPB12 in Table 1 of Ref. [28]). Therefore, we examined the viscosity results particularly closely for these



Scheme 1. Preparation of Functionalized 1250k 1,4-Polybutadiene Molecules Used in the Present Study: Thiol-Ene Addition of (a) 3-Mercaptopropionic Acid [26], and (b) Dimethylaminoethane thiol Hydrochloride.

polymers. Although the amine functionalized polymer 1250k1.5N had specific viscosity identical to that of the parent polymer 1250kPB (e.g., $\eta_0 = 3.0$ mPa s for both polymers at the overlap concentration of 2500 ppm at 25 °C in Jet-A), a small amount of crosslinking appears to have occurred in the preparation—possibly during workup—of 1250kPB2.6N and 1250kPB5.4N (e.g., η_0 at c^* for these polymers was 7% and 30% greater than for the prepolymer, respectively; we note that this effect cannot be attributed to side-group associations, since tertiary amines do not self-associate).

Thus, we conclude that the modification of the general functionalization procedure [28] to accommodate the ionic character of DMAET may have compromised the faithful preservation of the prepolymer's narrow MW distribution (see Appendix A for other studies regarding the change in molar mass distribution of 1,2-PB upon addition of DMAET). Nevertheless, the small changes in polydispersity that may be present in the 1250kPBxxN series do not affect the conclusions of this study.

3.2. Phase behavior

As mentioned in the Introduction, solution properties (and in particular phase behavior) of functional polymers and of their complexes depend strongly on the nature of the solvent. The self-association of acid functionalized homologues in dodecane, chlorododecane (CDD), tetrachloroethane (TCE), and chloroform [26] have shown that small increases in solvent polarity greatly reduce the strength of H-bonds and, concomitantly, increase the single phase regime in the phase diagram as a function of polymer concentration and temperature. In relation to single-component solvents, Jet-A has character intermediate between CDD and TCE. Unlike a single component solvent, however, Jet-A refers to a mixture whose composition lies in a narrowly specified range. In the context of research for improved mist-suppression of aviation fuels, the use of Jet-A as a solvent introduces complications associated with multicomponent solvents (which may complicate the analysis of polymer solution behavior), as well as complications due to the presence of impurities of unknown nature and concentrations that may interfere with DA interactions. Fortunately, the salient effects of donor–acceptor interactions on phase separation, aggregate formation, and solution viscosity/elasticity are so pronounced that the added complexity associated with Jet-A does not mask the effect of DA interactions or compromise the conclusions of this study.

The degree of functionalization was kept low enough that the individual species dissolved to form homogenous solutions in Jet-A at 25 °C at all concentrations tested (up to 1.5 wt% polymer). Note that the temperature must be specified due to the strong effect of temperature on phase behavior (e.g., 1250kPB0.6A polymer separated into gel and sol phases in Jet-A at 0 °C at all concentrations tested). Based on solubility at 25 °C, the highest degrees of functionalization, per 100 butadiene units, were 5.4 tertiary amine side-groups and 0.6 carboxylic acid side-groups (Table 1). Although the

individual components of Table 1 formed single phase solutions at $T = 25$ °C and $c = 0.25$ wt%, for some pairs intermolecular associations of carboxylic acid and tertiary amine side-groups caused phase separation into polymer-rich (gel) and polymer-poor (sol) phases (Table 2). The amount of gel formed for a given polymer pair (at fixed temperature and total polymer concentration) was found to vary non-monotonically with the ratio $r_{N/A}$ of tertiary amine and carboxylic acid groups, reaching a maximum for $r_{N/A}$ close to 1.

We chose to conduct further examination of solution properties only for those pairs of polymers that did not phase separate (Table 2).

3.3. Aggregate formation and effects on shear viscosity

Dynamic light scattering measurements at 25 °C on mixtures of proton-donating MPA polymer and proton-accepting DMAET polymer at the dilute concentration of 1500 ppm revealed objects with hydrodynamic size greater than that of either of the individual components (Fig. 3a). In contrast, self-associating stickers did not themselves produce large (soluble) aggregates (see pure 1250kPBxxA results in Fig. 3). Formation of interpolymer aggregates even in the dilute regime in this and other studies reflects the expectation that the acid–base interaction dwarfs the strength of the self-association of the carboxylic acid donor groups. The size of (soluble) interpolymer complexes (Fig. 4) was found to increase with increasing total polymer concentration, so that significant increases in $\langle R_h \rangle$ could be achieved at concentrations as low as c^* (e.g., 3-fold increase at $c^* = 2500$ ppm for 1:1 wt. mixtures of 1250kPB0.2A and 1250kPB5.4N, Fig. 3b). These results accord with prior literature showing that donor–acceptor interactions can drive multiple chains to associate even in dilute solution [27,29].

At fixed sticker density on one partner (e.g., 1.5% N), increasing the sticker density on the other partner was observed to increase aggregate size, at least up to the limit imposed by phase separation. Notice that phase separation precludes simply increasing sticker density on both species as a means to promote larger aggregates: at a certain point, increasing the number density of stickers on one of the chains requires decreasing the number density of stickers on the partner chains in order to remain in the homogeneous regime. We found that the largest aggregates form when the extent of functionalization of one of the species is pushed up to its single-component solubility limit (i.e., mixtures of 1250kPB0.2A and 1250kPB5.4N, and mixtures of 1250kPB0.8A and 1250kPB1.5N gave the highest enhancement in $\langle R_h \rangle$ at both 1500 and 2500 ppm, Fig. 3).

For a given pair of acid-functionalized and base-functionalized polymers, we further observed that the largest soluble clusters were obtained in the vicinity of 1:1 weight ratios of the chains, in some cases far from 1:1 molar ratios of the stickers (where the tendency for phase separation is the most pronounced). The interpretation of this result, which held for all mixtures tested at both 1500 and 2500 ppm (Fig. 3), is that asymmetry in the number density of partner chains disrupts formation of large

Table 2
Phase behavior^a of and experiments^b conducted on mixtures of 1250kPB proton-donating and proton-accepting chains in Jet-A solvent.

	0.2% A	0.3% A	0.4% A	0.6% A
1.5% N				
2.6% N	CaBER	Drop Breakup		
5.4% N				

^a Hatched boxes indicate mixtures that phase separate at 25 °C and 0.25 wt% total polymer.

^b Shaded boxes correspond to mixtures for which solutions at 25 °C and 0.25 wt% total polymer were characterized using spray, shear, and light scattering experiments.

interpolymer complexes, at least for the case of matched chain lengths.

Our first observation about the effect of interactions on shear viscosity is that they have little effect on η_0 despite large changes in $\langle R_h \rangle$: for example, at the overlap concentration of 2500 ppm (Fig. 3b), the effect of donor–acceptor interactions increased η_0 less than 20% (excluding the mixture involving the measurably cross-linked 1250kPB5.4N), even though $\langle R_h \rangle$ changed up to 300% (Fig. 5). Thus, formation of large clusters did not result in commensurate shear viscosity enhancements (or extensional viscosity enhancements, as discussed in the next section).

Next, inspection of shear viscosity results at the overlap concentration of the 1250kPB shows that—in contrast to self-associating pairwise interactions—donor–acceptor interactions increase η_0 relative to unfunctionalized chains at c^* (whereas self

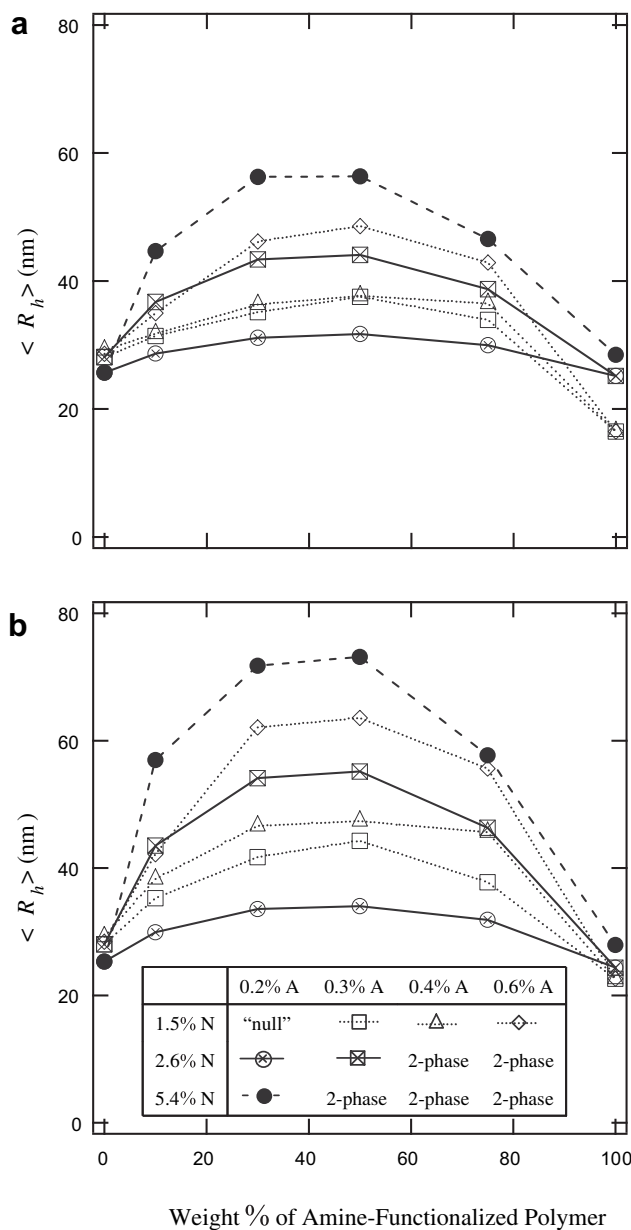


Fig. 3. Hydrodynamic radii of polymeric structures formed in mixtures of hydrogen-bond donor (1250kPBxxA) and acceptor (1250kPBxxN) chains in Jet-A at 25 °C as a function of the fraction (wt 1250kPBxxN)/(wt 1250kPBxxN + wt 1250kPBxxA) for total polymer concentrations of (a) 1500 ppm and (b) 2500 ppm.

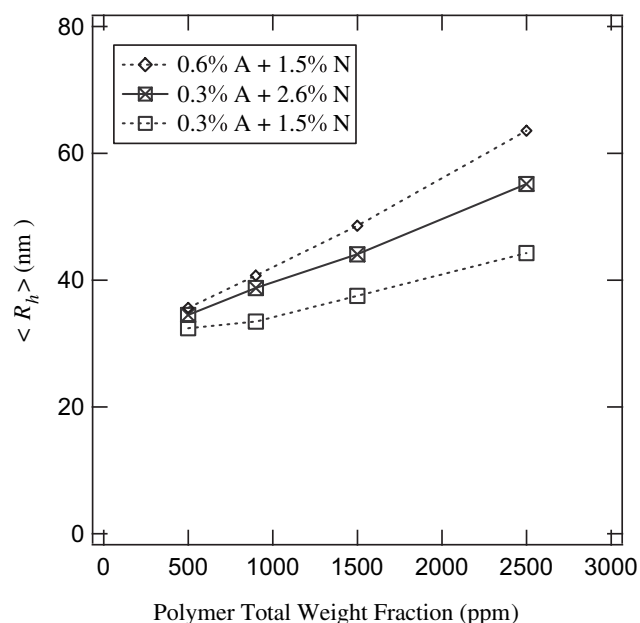


Fig. 4. Hydrodynamic radii at 25 °C of mixtures of proton-donating (1250kPBxxA) and proton-accepting (1250kPBxxN) chains in Jet-A, as a function of increasing total polymer concentration in the dilute regime.

associations lead to negative deviations in η_0 , as seen for the acid-functionalized molecules by themselves in Fig. 5). This indicates that in the self-associating case, the depression of η_0 due to chain collapse is greater than any positive enhancement in shear viscosity that may result from formation of polymer clusters [26]; in the donor–acceptor case the opposite holds. As concentration increases beyond c^* , interpolymer complex formation increases, manifested in greater positive deviations in solution shear viscosity. For example, at 1.5 wt% total polymer ($\approx 6c^*$), η_0 for mixtures of 1250kPB2.6N and 1250kPB0.2A in 15:85 and 30:70

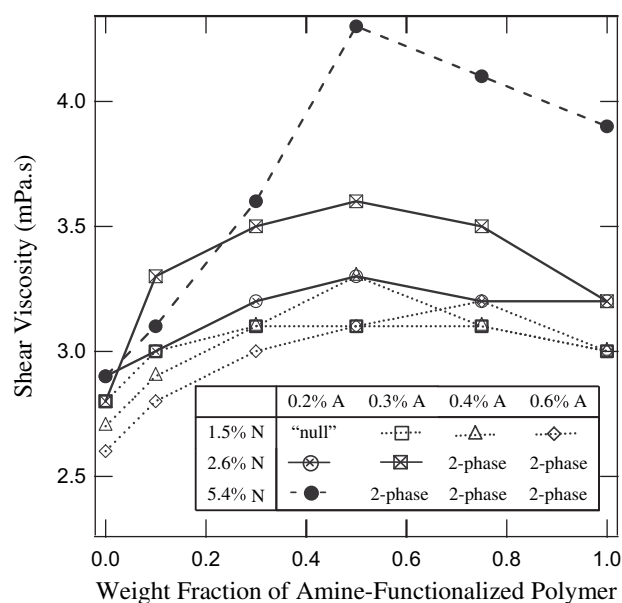


Fig. 5. Zero-shear viscosity (adjusted to two significant figures) at 25 °C of mixtures of proton-donating (1250kPBxxA) and proton-accepting (1250kPBxxN) chains in Jet-A at total polymer wt fraction of 2500 ppm, as a function of the fraction of amine-functionalized chains: (wt 1250kPBxxN)/(wt 1250kPBxxN + wt 1250kPBxxA). The viscosities of the solvent and of the 1250k 1,4-PB prepolymer at 2500 ppm in Jet-A were 1.4 and 3.0 mPa.s, respectively.

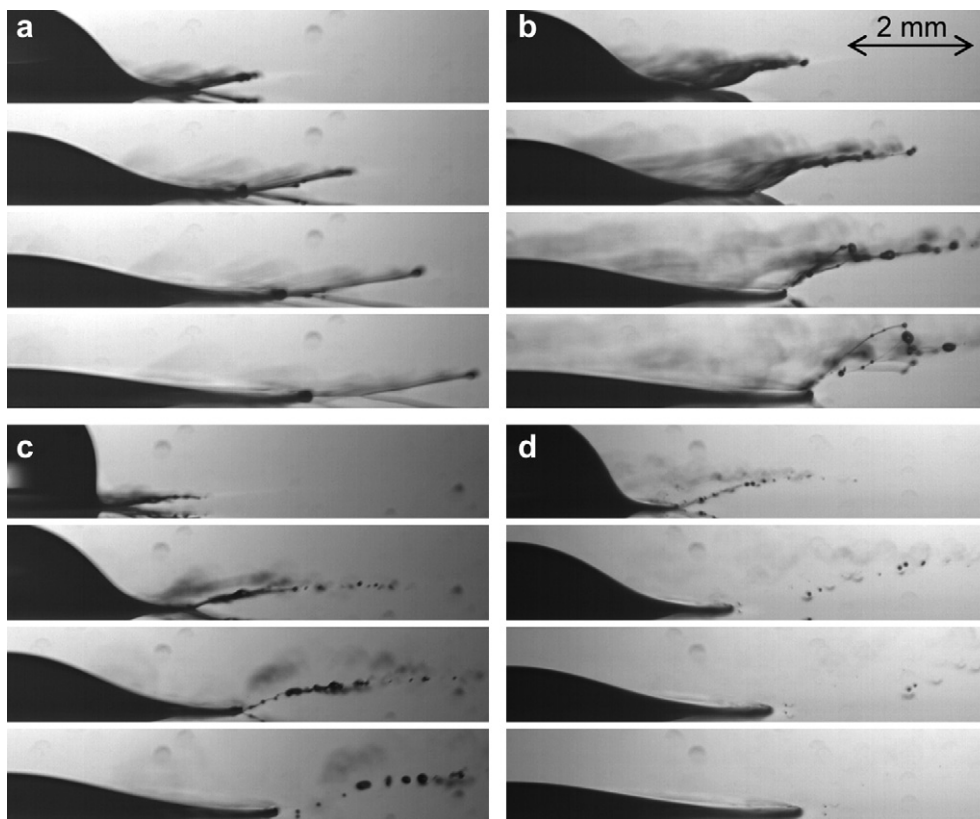


Fig. 6. High-speed imaging of drop breakup of polymer solutions at 180 ppm by wt in Jet-A at 25 °C: (a) 4200 kg/mol linear, non-associating polyisobutylene chains; (b) 1250 kg/mol linear, unfunctionalized 1,4-polybutadiene (PB) chains; (c) 1250kPB0.3A and 1250kPB2.6 N in 3:1 wt ratio; and (d) 1250kPB0.3A and 1250kPB2.6 N in 1:1 wt ratio (refer to Table 1). For 4200 kg/mol polyisobutylene, satellite droplets were never fully ejected; on the other hand all visible fluid filaments connecting “beads” of fluid together had broken 2 ms, 1 ms, and 0.5 ms after impact for solutions b, c, and d, respectively. The interval between frames is 0.25 ms in all cases. Experiments were performed in Prof. Albert Ratner’s laboratory at the University of Iowa.

wt ratios were 130 and 180 mPa s, respectively—two- to three-times greater than the viscosity of either individual component at this concentration (62 and 77 mPa s for 1250kPB0.2A and 1250kPB2.6N at 1.5 wt% in Jet-A, cf. 48 mPa s for 1250kPB prepolymer). Our observations are consistent with literature reports for comparable systems that the shear viscosity of donor/acceptor mixtures is greater than that of their non-associated components and increases non-linearly even in the dilute concentration regime [29–34]. In relation to fuel additives, the requirement that shear viscosity remain low combined with the growth of viscosity above c^* necessitates the design of associative polymers that are effective as mist-suppressing additives even in the dilute regime ($c \leq c^*$).

3.4. Elasticity and mist suppression

To evaluate the effect of donor–acceptor interpolymer associations in dilute solution, drop impact experiments (Fig. 6) were used to probe elasticity and drop breakup. As negative and positive controls, we used Jet-A and solutions of $> 4 \times 10^6$ g/mol PIB at 180 ppm in Jet A. In accord with prior literature on mist suppression by very long PIB [14], we found that 4200 kg/mol PIB at 180 ppm in Jet-A promotes formation of fluid filaments that suppress the ejection of satellite droplets (i.e., the fluid filaments seen in Fig. 6a simply settled next to the droplet), in sharp contrast to the rapid fragmentation of ejected fluid in the absence of polymer (Fig. 1a of Ref. [26]). Consistent with the well-known [13,14,36], pronounced effect of chain length on polymer elasticity, substantially more fluid is ejected for solutions of 1250 kg/mol polymer chains (corresponding to chain

lengths reasonably resistant to mechanical degradation in turbulent flow [8,37]). At 180 ppm of 1250 kg/mol PB (Fig. 6b), fluid filaments elongate and some drops escape, although polymer elasticity for these chains is sufficient to strongly alter the splashing and breakup processes, substantially increasing, for example, the size of ejected droplets (compare Fig. 6b and Fig. 1a of Ref. [26]).

We found that the ability of 1250kPB to suppress drop breakup was reduced by interpolymer complexation via DMAET and MPA associations: drop impact results at 180 ppm (Fig. 6c and 6d) show little evidence of fluid filaments and the ejection of numerous fine droplets in patterns that resemble those obtained for pure Jet-A (compare Fig. 6d with Fig. 1a of Ref. [26]). Increasing concentration to 450 ppm enhanced suppression of breakup (Figure A.2 of Appendix A) for all four systems examined in Fig. 6, but their relative performance did not change. Indeed, at both concentrations, the lifetime of filaments connecting beads of fluid for the unfunctionalized parent polymer was reduced by $\frac{1}{2}$ for the 1250kPB0.3A and 1250kPB2.6N mixture in 3:1 wt ratio, and by $\frac{1}{4}$ for the same mixture in 1:1 wt ratio. Note that the solution with the largest aggregates, at 1:1 wt ratio of the chains (Figs. 3 and 4), was the least effective in suppression of drop breakup.

Thus, donor–acceptor interactions do not overcome the undesired reduction of the effect of polymer on drop breakup in dilute solutions that was observed earlier for self-associating systems. Indeed, comparison of Fig. 6 and Figure A.2 of Appendix A with Fig. 10 of Ref [26] reveals that the mist-suppression performance of the mixture of acid- and base-functionalized polymers was inferior to that of the acid-functionalized polymers by themselves, which were inferior to the unmodified prepolymer.

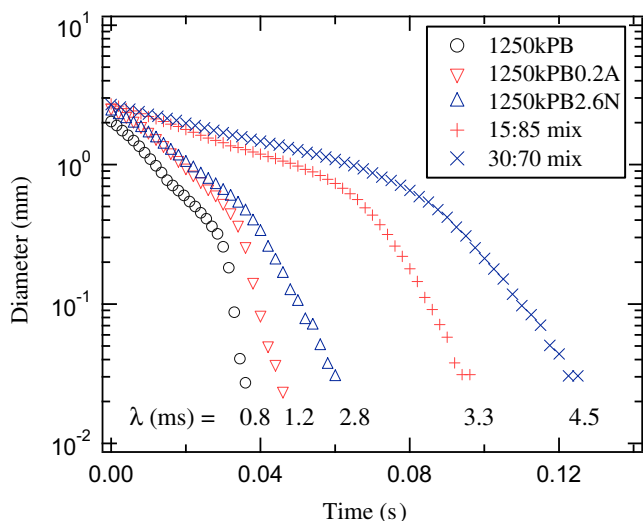


Fig. 7. Time evolution of filament diameter during capillary breakup experiments for mixtures of 1250k2.6N and 1250k0.2A polymers in 15:85 and 30:70 wt ratios, and for appropriate reference solutions, at 1.5 wt% total polymer content in Jet-A at 25 °C (corresponding to $c = 6c^*$ for 1250kPB prepolymer). All tests were performed with 8 mm diameter plates, at initial and final aspect ratios of 1.0 and 2.2, respectively. Note that although the sampling rate was 10 kHz in all cases, sparse data points are shown for clarity. Solution shear viscosities were 48, 62, and 77 mPa s for the 1250kPB, 1250kPB0.2A, and 1250kPB2.6N reference solutions, and 130 and 180 mPa s for the 85:15 and 70:30 mixtures, respectively. The characteristic relaxation times of the solutions, determined from the slope of the exponential decay of the filament diameter vs. time, are represented on the figure. Measurements were made at a Thermo Fischer Scientific laboratory with the assistance of Dr. Jan Plog.

Motivated by the strong concentration dependence of the physical properties of donor–acceptor interpolymer mixtures between the dilute and semi-dilute regimes, we examined the behavior at c^* and in the semi-dilute regime via spray and CaBER experiments. (As noted earlier, the drop impact experiment was limited to $c \ll c^*$).

Near the overlap concentration, the only applicable method was the spray experiment. Such experiments revealed surprisingly small differences in atomization as a result of donor–acceptor interpolymer associations at $c^* = 2500$ ppm (Fig. A.3–A.8 of Appendix A), despite a 2-fold variation in shear viscosity (Fig. 5) and 3-fold variation in hydrodynamic radius of clusters (Fig. 3b). In fact, in most cases, the

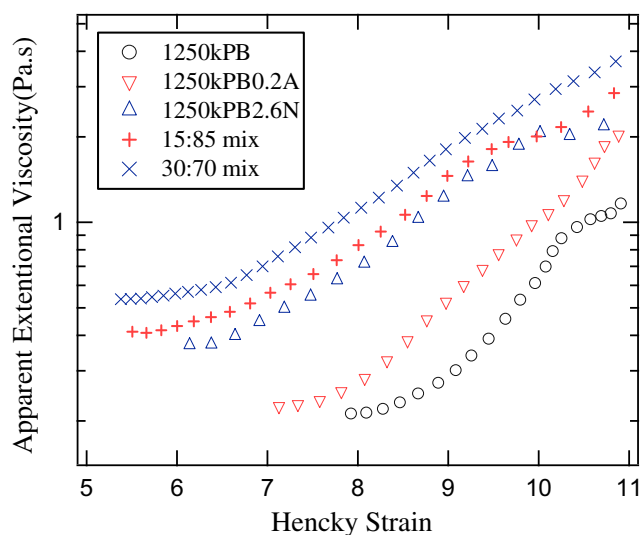


Fig. 8. Effect of acid–base complementary associations on apparent extensional viscosity during capillary breakup rheology (refer to Fig. 7 for experimental details).

size distribution of droplets generated in the spray experiment shifted to smaller values as a result of interpolymer complexation, as was the case for self-associating polymer systems [26].

Quantitative measurements of extensional viscosity and relaxation time (by capillary breakup rheometry) were possible for 1250kPB chains at $c \geq 1.5$ wt% (corresponding to $c \geq 6c^*$) in Jet-A. As mentioned in Section 2.3.3, solution elasticity was unfortunately too low to be measured at lower concentrations for this system. Attempts were made, without success, to enable CaBER experiments of dilute 1250 kg/mol PB by adding low molar mass polymer to increase the viscosity of the solvent (e.g., Jet-A containing 3–15 wt% 50–500 kg/mol polyisobutylene or polyisoprene). In all such attempts, either solution shear viscosity was still too low to enable elasticity measurements of the 1250 kg/mol PB solutions, or the functionalized 1250 kg/mol PB chains phase separated. CaBER results for mixtures of 1250kPB0.2A and 1250kPB2.6N polymers at 1.5 wt% show that intermolecular complexation increased solution relaxation time, apparent extensional viscosity, and breakup time of the filaments (Figs. 7 and 8). However, these increases matched precisely the increases in the shear viscosity of the solutions: intermolecular complexation did not enhance solution elasticity, relative to shear viscosity—even well into the semi-dilute concentration regime.

The observed effects of donor–acceptor polymer–polymer interactions on drop and capillary breakup are surprising in light of literature evidence [24,25,27] that interpolymer complexation produces large aggregates at and below c^* and results in enhanced viscosity, shear-thickening and drag-reduction (relative to non-associating and self-associating molecules). Based on the positive correlations between drag-reduction and mist-suppression (Appendix A), and between polymer size and mist suppression [13,14], the adverse effects of donor–acceptor complexation on drop breakup at $c \leq c^*$ are at odds with our expectations based on the state of prior understanding. These adverse effects indicate that, at low polymer concentrations, interchain associations, like intrachain associations [26], hinder the mechanism of mist-suppression despite the formation of large polymer clusters. We hypothesize that physical bonds inhibit stretching of the chains in extensional flow. This physical phenomenon persists at higher concentrations: in spite of large enhancements in shear viscosity (relative to both unfunctionalized and self-associating chains of the same length), donor–acceptor molecules showed a surprising lack of solution elasticity up to $c = 6c^*$ (Figs. 7 and 8).

4. Conclusion

The present contribution is part of an effort to understand molecular aspects of the rheology of pair-wise associating polymers and complements an earlier study of linear flexible chains bearing self-associating side groups. Therefore, we present unified experimental results regarding the effects of stickers on polymer solubility, polymer aggregation, solution viscosity, and elastic behavior in extensional deformation. In light of our earlier findings [26] that intra-chain associations dominate the solution properties of self-associating systems (Fig. 1a) even beyond the dilute concentration regime, we examined here donor–acceptor systems (Fig. 1b) in the hope that complementary associations would result in more favorable effects on polymer elasticity and superior properties for control of fluid breakup.

The effects of association in dilute solution were sufficiently subtle that it proved significant to perform properly controlled studies that compare functionalized and unmodified polymer homologues of matched length. To test previous concepts regarding correlations between cluster size and viscosity, it was useful to perform light scattering and rheological characterization on each

solution. The results did *not* support the usual correlations between polymer size and polymer elasticity. Although we found no mention of it in prior literature on the use of associative polymers as fuel additives, the strong reduction in solubility with addition of “stickers” proved significant, both in relation to single-component solutions and donor–acceptor mixtures.

These results provide new insight regarding the molecular effects of interchain associations randomly located along the chain on the dynamic polymer response in extensional deformation. Specifically, the success of donor–acceptor interactions in driving intermolecular associations in dilute solutions does not overcome the limitations of chain collapse observed earlier [26] for self-associating chains: within the multichain donor–acceptor clusters, the segment density is increased (the participating chains are relatively collapsed) and the ability of the chains to elongate in extensional flow is reduced. The implications of our studies for mist control of aviation fuel are that linear chains with randomly placed stickers—whether self-associating or donor–acceptor type—are inferior to non-associating polymer analogues even at concentrations several times c^* . Therefore, alternative strategies to improve antimisting using associative polymers are needed.

Acknowledgments

Funding for this research was provided by the FAA and NASA, the Caltech Milliken Foundation, and the Caltech Gates Grubstake Fund. We acknowledge the contributions of Brett F. Bathel and Prof. Albert Ratner (University of Iowa) in the drop breakup experiments and of Dr. Jan P. Plog (Thermo Fisher Scientific) in the CaBER experiments. We also thank Dr. Steven Smith of Proctor and Gamble Company for supplying the 1,2-PB precursor materials, and Dr. Suneel Kunamaneni for contributing the ideas that initiated the direction of this work.

Appendix. Supplementary data

Background information about the effect of polymer viscoelasticity on drag reduction and drop breakup, results of functionalization of 1,2-PB with DMAET, results of drop breakup experiments at 450 ppm for the solutions of Figure 6, and additional results of spray experiments for the mixtures specified in Table 2 are provided as supplementary information. Supplementary data associated with this article can be found in the online version, at doi:10.1016/j.polymer.2009.10.032.

References

- [1] Oliver DR, Bakhtiyarov SI. *Journal of Non-Newtonian Fluid Mechanics* 1983;12(1):113–8.
- [2] Lumley JL. *Annual Review of Fluid Mechanics* 1969;1:367.
- [3] Lumley JL. *Journal of Polymer Science Macromolecular Reviews* 1973; 7(1):263–90.
- [4] Bewersdorff HW, Berman NS. *Rheologica Acta* 1988;27(2):130–6.
- [5] Gadd GE. *Nature* 1965;206(4983):463.
- [6] de Gennes PG. *Introduction to polymer dynamics*. Cambridge University Press; 1990.
- [7] Sreenivasan KR, White CM. *Journal of Fluid Mechanics* 2000;409:149–64.
- [8] Brostow W. *Polymer* 1983;24(5):631–8.
- [9] Brostow W, Majumdar S, Singh RP. *Macromolecular Rapid Communications* 1999;20(3):144–7.
- [10] Min T, Jung YY, Choi H, Joseph DD. *Journal of Fluid Mechanics* 2003;486: 213–38.
- [11] Ptasiński PK, Boersma BJ, Nieuwstadt FTM, Hulsen MA, Van den Brule BHAA, Hunt JCR. *Journal of Fluid Mechanics* 2003;490:251–91.
- [12] Matthys EF. *Journal of Non-Newtonian Fluid Mechanics* 1991;38:313–42.
- [13] Anna SL, McKinley GH. *Journal of Rheology* 2001;45(1):115–38.
- [14] Chao KK, Child CA, Grens EA, Williams MC. *AIChE Journal* 1984;30(1): 111–20.
- [15] Christanti Y, Walker LM. *Journal of Rheology* 2002;46(3):733–48.
- [16] Mun RP, Byars JA, Boger DV. *Journal of Non-Newtonian Fluid Mechanics* 1998;74:285–97.
- [17] Smolinski JM, Gulari E, Manke CW. *AIChE Journal* 1996;42(5):1201–12.
- [18] Entov VM, Yarin AL. *Fluid Dynamics* 1984;19(1):21–9.
- [19] Goldin M, Yerushal J, Pfeffer R, Shinnar R. *Journal of Fluid Mechanics* 1969;38:689.
- [20] Gordon M, Yerushal J, Shinnar R. *Transactions of the Society of Rheology* 1973;17(2):303–24.
- [21] Christanti Y, Walker LM. *Journal of Non-Newtonian Fluid Mechanics* 2001;100:9–26.
- [22] Motier JF. *Hydrocarbon fuels containing antimisting agents*. 1986.
- [23] Knight J. *Antimisting additives for aviation fuels*. 1983.
- [24] Kowalik RM, Duvdevani I, Peiffer DG, Lundberg RD, Kitano K, Schulz DN. *Journal of Non-Newtonian Fluid Mechanics* 1987;24(1):1–10.
- [25] Schulz DN, Kitano K, Duvdevani I, Kowalik RM, Eckert JA. *ACS Symposium Series* 1991;462:176–89.
- [26] David RLA, Wei M-H, Liu D, Bathel BF, Plog JP, Ratner A, et al. *Macromolecules* 2009;42(4):1380–91.
- [27] Malik S, Mashelkar RA. *Chemical Engineering Science* 1995;50(1):105–16.
- [28] David RLA, Kornfield JA. *Macromolecules* 2008;41(4):1151–61.
- [29] Xiang ML, Jiang M, Zhang YB, Wu C, Feng LX. *Macromolecules* 1997;30(8): 2313–9.
- [30] Qi GR, Wang YH, Li XX, Peng HY, Yang SL. *Journal of Applied Polymer Science* 2002;85(2):415–21.
- [31] Wang YH, Qi GR, Li HL, Yang SL. *European Polymer Journal* 2002;38(7):1391–7.
- [32] Wang YH, Qi GR, Peng HY, Yang SL. *Polymer* 2002;43(9):2811–8.
- [33] Qiu XP, Jiang M. *Polymer* 1994;35(23):5084–90.
- [34] Qiu XP, Jiang M. *Polymer* 1995;36(18):3601–4.
- [35] Jiang M, Li M, Xiang ML, Zhou H. *Interpolymer complexation and miscibility enhancement by hydrogen bonding*. *Polymer synthesis polymer-polymer complexation*, vol. 146. Berlin: Springer-Verlag Berlin; 1999. p. 121–196.
- [36] Yu JH, Fridrikh SV, Rutledge GC. *Polymer* 2006;47(13):4789–97.
- [37] Motier JF. Personal communication to the authors, 2006.